

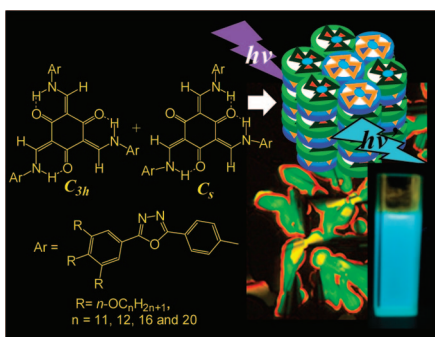
**Luminescent, Liquid Crystalline
Tris(*N*-salicylideneaniline)s: Synthesis and
Characterization**

Channabasaveshwar V. Yelamaggad,*
Ammathnadu S. Achalkumar, D. S. Shankar Rao, and
S. Krishna Prasad

Centre for Liquid Crystal Research,
Jalalhalli, Bangalore 560013, India

yelamaggad@gmail.com

Received January 30, 2009



A new class of discotics derived from tris(*N*-salicylideneaniline)s have been synthesized and their thermal and photophysical properties are investigated. These systems with outer 1,3,4-oxadiazole wings exist in an inseparable mixture of two keto-enamine tautomeric forms with C_{3h} and C_s rotational symmetries, and self-assemble into fluid columnar phase over a wide thermal range as evidenced by several complementary studies. They possess emissive characteristics in both solution and columnar states; the blue light ($\lambda = 474$ nm) emission has been evidenced for the former state.

The design, fabrication, and optimization of efficient light emitting diodes (LEDs) based on organic materials is one of the thrust areas of research due to the promising applications in flat-panel displays.¹ The vital factor for the successful development of organic light emitting devices (OLEDs) is the molecular engineering and synthesis of stable emissive organic compounds associated with desired properties. Thus, a wide range of materials varying from the low molar mass materials to processable polymers^{2,3} have been realized to examine their suitability for OLEDs. Of these, the structurally diverse functional single molecules with the ability to form LC phases

* To whom correspondence should be addressed.

(1) (a) Kelly, S. M. In *Flat Panel Displays: Advanced Organic Materials*; RSC Materials Monographs; Royal Society of Chemistry: Letchworth, UK, 2000. (b) Kraft, A.; Grimsdale, A. C.; Holmes, A. B. *Angew. Chem., Int. Ed.* **1998**, *37*, 402–428. (c) Hoga, B. P.; Gin, D. L. *Liq. Cryst.* **2004**, *31*, 185–199, and references cited therein.

have been attracting special attention as they combine the unique feature of self-assembly and intrinsic light emitting capabilities that are promising in emissive LC displays⁴ and anisotropic OLEDs.⁵ This is especially striking in the case of columnar (Col) phases of disk-shaped (discotic) LCs, in which the aromatic cores stack on top of one another and the columns thus formed possess two-dimensional (2D) lattice. The strong π - π interaction and thus the thorough overlap of the frontier orbitals of the aromatic cores enables the facile charge migration along the columns, a fundamental feature required for the OLED functioning. Specifically, they can be used as components of OLEDs such as hole transport (p-type), electron transport (n-type), and emissive layers.¹ Besides the economic feasibility, ease of processability, self-healing of structural defects, and the possibility to tune their properties make the Col phases very attractive. Indubitably, Col phases are gaining acceptance as substitutes for single crystals or conjugated polymers that are used in electronic devices such as OLEDs,⁵ photovoltaic cells, and field effect transistors.⁶

In this context, tris(*N*-salicylideneaniline)s (TSANs),^{7–9} a novel class of compounds existing as a mixture of C_{3h} and C_s symmetric keto-enamine tautomers, are promising as they readily offer induction and tuning of both electronic, viz. luminescence, as well as molecular material features like self-organizing ability, molecular recognition, etc.^{7–9} For example, based on the work of McLachlan et al., we have recently demonstrated that by the space-filling approach TSANs can be made to stabilize Col phase(s).^{8a} In a later study, we noted that these materials possess some promising inherent electronic (fluorescence) property in solutions.^{8b,c} Interestingly, other studies have disclosed that the electronic properties of TSANs, in particular the C_{3h} isomer, can be effectively altered by changing their peripheral substitutions; Lee et al. have deter-

(2) (a) Heeger, A. J.; Diaz-Garcia, M. A. *Curr. Opin. Solid Phys. Mater. Sci.* **1998**, *3*, 16–22. (b) Friend, R. H.; Gymer, R. W.; Holmes, A. B.; Burroughes, J. H.; Marks, R. N.; Taliani, C.; Bradley, D. D. C.; dos Santos, D. A.; Bredas, J. L.; Logdlund, M.; Salaneck, W. R. *Nature* **1999**, *397*, 121–128. (c) Molenkamp, W. C.; Watanabe, M.; Miyata, H.; Tolbert, S. H. *J. Am. Chem. Soc.* **2004**, *126*, 4476–4477.

(3) (a) Tang, C. W.; Van Slyke, S. A. *Appl. Phys. Lett.* **1987**, *51*, 913–915. (b) Shi, J.; Tang, C. W. *Appl. Phys. Lett.* **1997**, *70*, 1665–1667. (c) Hung, L. S.; Chen, C. H. *Mater. Sci. Eng., R* **2002**, *39*, 143.

(4) Beer, A.; Scherowsky, G.; Owen, H.; Coles, H. *Liq. Cryst.* **1995**, *19*, 565, and references cited therein.

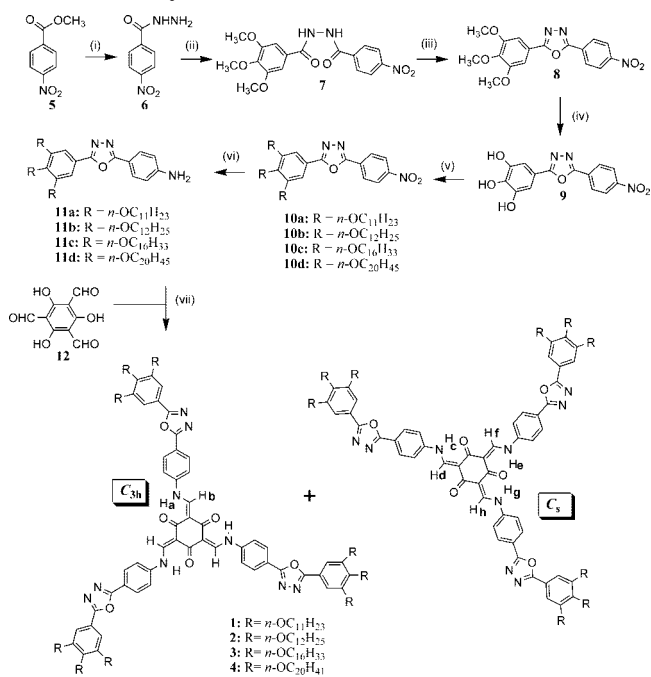
(5) Christ, T.; Glusen, B.; Greiner, A.; Kettner, A.; Sander, R.; Stumpf, V.; Tsukruk, V.; Wendorff, J. H. *Adv. Mater.* **1997**, *9*, 48.

(6) (a) Adam, D.; Schuhmacher, P.; Simmerer, J.; Hayssling, L. K.; Siemensmeyer, K. H.; Eitzbach, H.; Ringsdorf, Haarer, D. *Nature* **1994**, *371*, 141–143. (b) Osburn, E. J.; Schmidt, A. L.; Chau, K.; Chen, S. Y.; Smolenyak, P.; Armstrong, N. R.; O'Brian, D. F. *Adv. Mater.* **1996**, *8*, 926–928. (c) Schmidt-Mende, L.; Fechtenkötter, A.; Mullen, K.; Moons, E.; Friend, R. H.; MacKenzie, J. D. *Science* **2001**, *293*, 1119–1126. (d) Kumar, S. *Chem. Soc. Rev.* **2006**, *35*, 83–109.

(7) (a) Chong, J. H.; Sauer, M.; Patrick, B. O.; MacLachlan, M. J. *Org. Lett.* **2003**, *5*, 3823–3826. (b) Sauer, M.; Yeung, C.; Chong, J. H.; Patrick, B. O.; MacLachlan, M. J. *J. Org. Chem.* **2006**, *71*, 775–788.

(8) (a) Yelamaggad, C. V.; Achalkumar, A. S.; Rao, D. S. S.; Prasad, S. K. *J. Am. Chem. Soc.* **2004**, *126*, 6506–6507. (b) Yelamaggad, C. V.; Achalkumar, A. S. *Tetrahedron Lett.* **2006**, *47*, 7071–7075. (c) Yelamaggad, C. V.; Achalkumar, A. S.; Rao, D. S. S.; Prasad, S. K. *J. Org. Chem.* **2007**, *72*, 8308–8318.

(9) (a) Riddle, J. A.; Bollinger, J. C.; Lee, D. *Angew. Chem., Int. Ed.* **2005**, *44*, 6689–6693. (b) Riddle, J. A.; Lathrop, S. P.; Bollinger, J. C.; Lee, D. *J. Am. Chem. Soc.* **2006**, *128*, 10986–10987. (c) Jiang, X.; Bollinger, J. C.; Lee, D. *J. Am. Chem. Soc.* **2006**, *128*, 11732–11733.

SCHEME 1. Synthesis of Oxadiazole-Based TSANs^a

^a Reagents and conditions: (i) ethanol, hydrazine hydrate, reflux °C, 1 h (90%); (ii) 3,4,5-trimethoxybenzoyl chloride, pyridine, 60 °C, 12 h (75%); (iii) POCl₃, 100 °C, 5 h (70%); (iv) BBr₃, CH₂Cl₂, -78 °C to rt, 17 h (65%); (v) *n*-bromoalkane, anhydrous K₂CO₃, DMF, 80 °C, 17 h (80–85%); (vi) 10% Pd–C, H₂ (balloon, 1 atm) THF, rt, 12 h (80–82%); (vii) ethanol, reflux, 6 h (65–75%).

mined that stereoelectronic control of self-assembly of C_{3h} isomers can enhance their fluorescence efficiency in solutions. These studies inspired us to incorporate a fluorophore in TSANs to possibly modify their luminescence characteristics while retaining the desired mesomorphism. The 1,3,4-oxadiazole was the obvious option given the fact that it shows promising electron transport and emission characteristics when used in OLEDs either as a dopant or as a part of another molecular system.¹⁰ Thus, the oxadiazole moiety in TSANs is expected to tune not only the emissive property but also the electron carrier (n-type) characteristics. We report here the synthesis and characterization of discotic TSANs **1–4** comprised of 1,3,4-oxadiazole cores.

The synthetic strategy to achieve these novel discotic TSANs bearing 1,3,4-oxadiazole fluorophores is illustrated in Scheme 1. Methyl 4-nitrobenzoate (**5**) was reacted with hydrazine hydrate in refluxing ethanol to obtain the hydrazide **6** that on treatment with 3,4,5-trimethoxybenzoyl chloride in the presence of pyridine furnished *N*-benzoylbenzohydrazide **7**. Phosphoryl trichloride-mediated cyclization of **7** yielded the trimethoxy oxadiazole derivative **8**,¹¹ which on demethylation with BBr₃ at -78 °C furnished the key precursor, namely, 2-(4-nitrophenyl)-5-(3,4,5-trihydroxyphenyl)-1,3,4-oxadiazole (**9**), in 65% yield. Compound **9** on *O*-alkylation with *n*-alkyl bromides under Williamson's ether synthesis condition yielded the nitro compounds **10a–d**, which on catalytic hydrogenation provided the requisite vital anilines **11a–d**. To our knowledge, compounds **9–11** were unknown hitherto, and are promising for realizing

TABLE 1. Transition Temperatures (°C)^a and enthalpies (kJ mol⁻¹) of the TSANs **1–4**

TSANs (C _{3h} :C _s) ^b	phase sequence ^d	
	heating	cooling
1 (1:2.9)	Cr 212.6 (7.3), Col ^c	
2 (1:2.5)	Cr 157.4 (13.4), Col _h ^c	
3 (1:2.6)	Cr ₁ 63.4 (131.6), Cr ₂ 157.3 (29.4), I 265.7 (4.9), Col _h	265.7 (4.9), Col _h
		24.6 (51.5), Cr
4 (1:2.7)	Cr ₁ 71.4 (122), Cr ₂ 115.2 (28.6), I 111.3 (23.7), Col _h	111.3 (23.7), Col _h
		64.7 (128), Cr

^a Phase transition temperatures (°C) and corresponding enthalpies (J/g) obtained from DSC thermograms during first heating and cooling cycles. ^b Ratio obtained from ¹H NMR. ^c The clearing temperature could not be detected in both POM and DSC as it exceeds 300 °C. ^d Cr, Cr₁ Cr₂ = crystal, Col_h = columnar hexagonal phase, I = isotropic phase.

a wide verity of luminescent LCs in the future. Finally, the reaction of anilines with 1,3,5-triformylphloroglucinol (**12**) afforded TSANs **1–4**. The pure yellowish solids were characterized by routine spectroscopic methods coupled with elemental analyses.

¹H NMR spectra of TSANs **1–4** revealed that they exist in two inseparable keto-enamine tautomeric forms having C_{3h} and C_s symmetries, as expected. In particular, the spectra showed multiple peaks between 8.8–9 and 13.1–13.6 due to coupling between enamine (vinylic: H_b, H_d, H_f, and H_h) and secondary amine (NH: H_a, H_c, H_e, and H_g) protons (see Table 1).¹² In principle, the measure of the area under the peaks (the integration) of H_a against H_c, H_g, and H_e of amine protons or H_b vs. H_d, H_f, and H_h can be considered to adjudge the ratio of two forms. However, owing to the close proximity of chemical shifts of enamine protons, we have considered amine protons for estimating the ratio of the two geometrical isomers (shown in Table 1). The coupling between the enamine and the NH protons was further confirmed by the ¹H–¹H COSY NMR spectra.¹²

Furthermore, the strong coupling (³J_{HH} ≈ 13 Hz)¹² elucidates the localization of the proton on the nitrogen atom. The phase behavior of the synthesized TSANs **1–4** was established with the aid of a polarizing optical microscope (POM), a differential scanning calorimeter (DSC), and X-ray diffraction (XRD). The sample placed between a clean untreated glass slide and a coverslip was used for the POM study. The preliminary mesophase assignment was based on the two inherent properties displayed by mesogenic TSANs: the birefringence and fluidity. The signatures observed in DSC thermograms due to phase transitions of all the samples were consistent with those of the optical experiments. In general, the phase transition temperatures deduced from calorimetric measurements of the first heating and cooling cycles at a rate of 5 deg/min are considered. However, when the thermal signatures were not observed in DSC thermograms, the transition temperatures were taken from the microscopic observations. A summary of the results deduced from these complementary techniques has been presented in Table 1.

In the microscopic study, the solid compounds **1** and **2** were observed to clearly melt into an identical mesomorphic state at 213 and 158 °C, respectively, showing birefringent homogeneous fluid (easily shearable) patterns that remained unaltered until about 300 °C (experimental limitation). On subsequent cooling of the samples, no textural change was observed except

(10) (a) Adachi, C.; Tsutui, T.; Saito, S. *Appl. Phys. Lett.* **1990**, *56*, 799. (b) Antoniadis, H.; Inbasekaran, M.; Woo, E. P. *Appl. Phys. Lett.* **1998**, *73*, 3055.

(11) Radha Vakula, T.; Saraswathi, T. V.; Srinivasan, V. R. *Indian J. Chem.* **1968**, *6*, 172–173.

(12) See the Supporting Information.

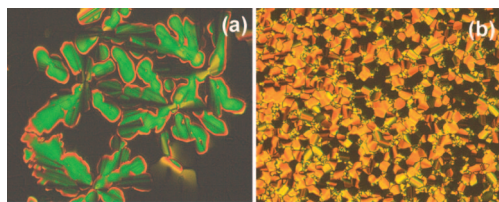


FIGURE 1. Photomicrographs of textures observed under POM of the Col_h phases of **3** at 258 °C (a) and **4** at 78 °C (b).

TABLE 2. The Results of Indexation of XRD Profiles of TSANs

TSAN	phase ^b T/°C	d ^a /Å	intensity ^c	lattice parameters/Å	Miller indices hkl
2	Col _h 200	40.6	s	a: 46.82	100
		4.8	d		
3	Col _h 230	42.9	s	a: 49.57	100
		4.9	d	c: 3.64	
		3.64	d		001
		47.4	s	a: 54.77	100
4	Col _h 90	4.5	d	c: 3.44	
		3.44	d		001
		48.3	s	a: 55.82	100
		27.8	s	c: 3.39	110
		4.6	d		
		3.39	d		001

^a d is spacing. ^b Col_h: hexagonal columnar phase. ^c s: strong, d: diffuse.

that mechanical shearing was not possible near room temperature. These transitions were highly reproducible, implying that these TSANs are chemically and thermally stable. As expected, for both compounds, DSC thermograms showed only a signature due to transition from the crystalline phase into the mesophase during the first heating cycle, while no peaks were detected in the successive cooling cycle or subsequent heating/cooling scans, which imply that the mesophase is glassy in nature at room temperature. Notably, the mesophases of **1** and **2** could be mixed well with the LC phases formed by TSANs **3** and **4**, which we shall discuss later, clearly indicating that all of them show an identical mesophase. Compounds **3** and **4** having longer alkyl chains were found to display an enantiotropic and a monotropic mesophase, respectively, with lower transition temperatures. On heating, the solid TSAN **3** melted (at 158 °C) into a mesophase with the nonspecific textural features identical to ones seen for **1** and **2** and remaining unaltered until the isotropic phase (270 °C). On subsequent cooling, it showed fan-shaped defects interspersed with large homeotropic domains (Figure 1a), features characteristic of the Col phases. The material crystallizes at 24 °C. The DSC thermograms¹² showed peaks at temperatures corresponding to those noted in the microscopic study. It may be mentioned here that the LC phase freezes if the sample is cooled slowly (about 1 deg/min). As mentioned above, TSAN **4** displayed a monotropic phase having a mosaic textural pattern as shown in Figure 1b. Thus, the longer (icosyl) chain of **4** effectively reduces the transition temperatures at the expense of mesophase stability. The high melting points of other TSANs can be attributed to the strong intermolecular association due to the large electrical dipole moment of the oxadiazole moiety.

The structural assignment of the Col phase formed by TSANs **2**, **3**, and **4** was achieved by X-ray diffraction study.¹² The results of indexing of one-dimensional (1D) intensity vs. 2θ profile deduced from the powder 2D pattern of the Col phases at different temperatures are summarized in Table 2. Except for TSAN **4**, all the diffractograms showed only a sharp Bragg (10)

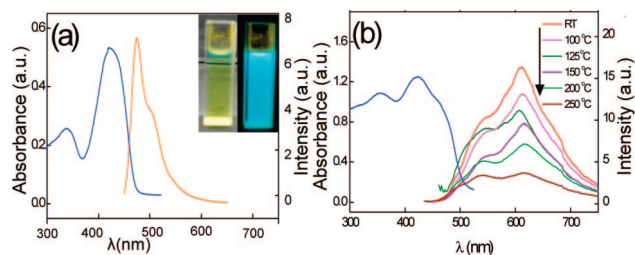


FIGURE 2. (a) Absorption spectrum (blue trace) and emission spectrum (orange trace) (excited at 420 nm) obtained for TSAN **3** in THF solution (2.3×10^{-6} M); the inset shows the pictures of solutions as seen before (left hand side (LHS)) and after the illumination (right hand side (RHS)) of 365 nm light. (b) Thin film absorption spectrum (LHS) at room temperature and emission spectra (RHS) for the thin film as a function of temperature.

peak in the low-angle region; the absence of expected multiple reflections for the Col phase can be ascribed to a minimum in the form factor. This is analogous to several reports wherein such a pattern has been assigned to a hexagonal columnar phase (Col_h).¹³ Although the presence of a single maximum at low angles does not allow for an unambiguous determination of the mesophase structure, the microscopic textures are consistent with a uniaxial, hexagonal columnar structure. It may be mentioned that the lattice constant *a* and not the *d*₁₀ spacing, which is comparable to the diameter of the molecule (determined with Chem3D Ultra 9), supports the argument that the structure is hexagonal columnar. In the wide-angle region, except for TSAN **2**, two broad reflections were observed. The first maximum corresponding to a spacing in the range of 4.5–4.9 Å is associated with the liquid-like correlation of the discs within the column. The second reflection indexed as (001) in the range of 3.4–3.6 Å indicates the periodic stacking, although short ranged, of the molecular cores within the column. Thus, the X-ray data coupled with the textural patterns suggest that the mesophase is indeed the Col_h phase. In the case of TSAN **4**, the X-ray evidence is more unambiguous with the existence of a second peak at low angles; the ratio of the spacings of the low angle reflections is 1:(1/√3), a feature expected for the Col_h phase.

As discussed before, owing to the presence of multiple chromophores and possible π-conjugations between the peripheral region and the central core, this series of discotic TSANs are expected to exhibit promising photophysical properties. The absorption and emission characteristics of these compounds were probed by using their solutions in tetrahydrofuran (10^{-6} M).¹² Figure 2a shows the combined UV–vis absorption and photoluminescent (PL) spectra of TSAN **3** as a representative case. The absorption spectrum (see the blue trace in Figure 2a) shows two bands around 353 and 438 nm attributed to the π–π* and n–π* transitions. Interestingly, upon irradiation with light of 420 nm, a sharp emission line in the blue region with a shoulder (at 498 nm) was obtained (474 nm; orange trace). This is remarkable given the fact that the blue light emitting materials

(13) (a) Alvarez, L.; Barbera, J.; Puig, L.; Romero, P.; Serrano, J. L.; Sierra, T. *J. Mater. Chem.* **2006**, *16*, 3768–3773. (b) Hayer, A.; de Halleux, V.; Kohler, A.; El-Garouhy, A.; Meijer, E. W.; Barbera, J.; Tant, J.; Levin, J.; Lehmann, M.; Gierschner, J.; Cornil, J.; Geerts, Y. H. *J. Phys. Chem. B* **2006**, *110*, 7653. (c) Barbera, J.; Gimenez, R.; Serrano, J. L. *Chem. Mater.* **2000**, *12*, 481, and references cited therein. (d) Carfagna, C.; Roviello, A.; Sirigu, A. *Mol. Cryst. Liq. Cryst.* **1985**, *122*, 151. (e) Gramsbergen, E. F.; Hoving, H. J.; de Jeu, W. H.; Praefcke, K.; Kohne, B. *Liq. Cryst.* **1986**, *1*, 397. (f) Metersdorf, H.; Ringsdorf, H. *Liq. Cryst.* **1989**, *5*, 1757. (g) Zeng, H.; Carroll, P. J.; Swager, T. M. *Liq. Cryst.* **1993**, *14*, 1421. (h) Artal, M. C.; Toyne, K. J.; Goodby, J. W.; Barbera, J.; Photinos, D. J. *J. Mater. Chem.* **2001**, *11*, 2801–2807.

TABLE 3. Photophysical Properties of TSAN 3

state	absorption/nm	emission ^b /nm	Stoke's shift
solution (THF) ^a	353, 438	474, 498 sh	36
glassy film (at rt)	350, 418	545 sh, 610	192

^a 10⁻⁶ M solution. ^b Excitation wavelength 420 nm; sh = shoulder.

are not only scarce but also their energy levels are high, and provide an effective approach in fine-tuning wavelength of emission on combining with another dopant emitter.^{10,14} Furthermore, the absorption–emission behavior of the fluid Col phase as well as its frozen state in the form of thin film was studied for TSAN 3 as a representative case. The substance held between the two coverslips was heated to isotropic phase, then cooled slowly until room temperature. Figure 2b illustrates the absorption of the frozen Col phase as well as the PL spectra of the Col structure at different temperatures starting from room temperature. The UV–vis spectrum of the film at room temperature shows two absorption bands at 350 and 418 nm similar to solution spectrum. On excitation (420 nm), the film showed a broad emission band at 610 nm (Stokes shift ca. 192 nm) with a shoulder at 545 nm (see Table 3). This large red shift can be attributed to the strong intermolecular interactions within the structure as well as the thickness of the sample. Therefore, for very thin (spin coated or vacuum deposited) samples there is the possibility that emission might shift toward the blue region. It can be seen that the fluorescence intensity decreases with the increase in the temperature indicating the breaking-up of the large stacks and thermally activated radiationless processes.¹⁵ Thus, the emissive frozen Col phase of TSANs characterized by the preserved 2D order and the short intracolumnar distance that facilitates motion of charges with impounding motion of the ionic impurities¹⁶ are promising in optoelectronic applications.

In conclusion, the synthesis, thermal behavior, and qualitative photophysical property of TSANs appended with 1,3,4-oxadiazoles are reported. Their solutions and fluid columnar phases facilitated by the self-assembly of two different geometrical

(14) (a) Tao, S.; Peng, Z.; Wang, P.; Lee, C.-S.; Lee, S.-T. *Adv. Funct. Mater.* **2005**, *15*, 1716–721. (b) Hu, N.-X.; Esteghamatian, M.; Xie, S.; Popovic, Z.; Hor, Ah.-M.; Beng, O.; Wang, S. *Adv. Mater.* **1999**, *11*, 1460–1463.

(15) Gimenez, R.; Pinol, M.; Serrano, J. L. *Chem. Mater.* **2004**, *16*, 1377–1383.

(16) Percec, V.; Glodde, M.; Bera, T. K.; Miura, Y.; Shiyonovskaya, I.; Singer, K. D.; Balagurusamy, V. S. K.; Heiney, P. A.; Schnell, I.; Rapp, A.; Spiess, H.-W.; Hudson, S. D.; Duank, H. *Nature* **2002**, *419*, 384–387.

forms exhibit emissive characteristics. Notably, solutions show blue fluorescence, while glassy Col film shows preserved emission behavior and 2D order. Thereby, we have disclosed a simple way of modifying molecular self-assembling and light-generating ability of TSANs. Importantly, some novel oxadiazole-based intermediates have been synthesized, which could be useful in the synthesis of light emitting liquid crystals.

Experimental Section

All the TSANs were synthesized following the experimental procedure described below for the TSAN 1 as a representative case. The preparation of all the intermediates and other TSANs and instrumentation are given in the Supporting Information.

A mixture of triformylphloroglucinol (0.005 mmol, 1 equiv) and aniline 11a (0.19 mmol, 3.4 equiv) in absolute ethanol (50 mL) was heated to reflux under inert atmosphere for 6 h with vigorous stirring. The dull yellow solid that separated upon cooling the reaction mixture was collected by filtration, repeatedly washed with ethanol, and air-dried. The crude product was purified by repeated recrystallizations in a mixture of absolute ethanol–THF (9:1) to obtain 1. *R_f* 0.54 (40% EtOAc–hexanes); an orange solid; yield 75%; UV–vis λ_{\max} = 425.94 nm, ϵ = 12.9239 × 10⁴ L mol⁻¹ cm⁻¹; IR (KBr pellet) ν_{\max} 2922, 2852, 2359, 1627, 1599, 1492, 1457, 1290, 1255, 1180, 1117, 1009, 838, 773, and 739 cm⁻¹; ¹H NMR (CDCl₃, 400 MHz) δ 13.57 (d, *J* = 13.0 Hz, =CNH), 13.51 (d, *J* = 13.1 Hz, =CNH), 13.2 (d, *J* = 12.9 Hz, =CNH), 8.82–8.95 (m, 3H, =CHN), 8.14–8.16 (m, 6H, Ar), 7.49 (t, 6H, *J* = 8.9 Hz, Ar), 7.32 (s, 6H, Ar), 4.02–4.1 (m, 18H, 9 × OCH₂), 0.87–1.86 (m, 189H, 81 × CH₂, 9 × CH₃). Anal. Calcd for C₁₅₀H₂₃₁N₉O₁₅: C, 75.05; H, 9.7; N, 5.25. Found: C, 75.23; H, 9.28; N, 4.91.

Acknowledgment. Prof. Suresh Das and Dr. Shibu Abraham, RRL, Trivendrum, and Prof. Uday Maitra and Mr. Nonappa, IISc, Bangalore, are gratefully acknowledged for providing their instruments to carry out the luminescence experiments and useful discussions.

Supporting Information Available: General information, experimental details, instrumentation, structural characterization data of all compounds, ¹H NMR spectra of compounds 1–4, 8, 9, 10c, and 11c, ¹H–¹H COSY NMR spectra of TSAN 3, one-dimensional intensity vs. 2 θ profiles of TSANs 2–4, DSC traces of TSAN 3, and absorption and emission spectra of TSANs 1–3. This material is available free of charge via the Internet at <http://pubs.acs.org>.

JO9001933